Author/s:
Zhang, X;Rayner, PJ;Wang, YP;Silver, JD;Lu, X;Pak, B;Zheng, X

Title:
Linear and nonlinear effects of dominant drivers on the trends in global and regional land carbon uptake: 1959 to 2013

Date:
2016-02-28

Citation:
Zhang, X., Rayner, P. J., Wang, Y. P., Silver, J. D., Lu, X., Pak, B. & Zheng, X. (2016). Linear and nonlinear effects of dominant drivers on the trends in global and regional land carbon uptake: 1959 to 2013. Geophysical Research Letters, 43 (4), pp.1607-1614. https://doi.org/10.1002/2015GL067162.

Submission for *Geophysical Research Letters*



# Linear and nonlinear effects of dominant drivers on the trends in global and regional land carbon uptake: 1959 to 2013

Xuanze Zhang[1, 2, 3], Peter J. Rayner[2], Ying Ping Wang[3], Jeremy D. Silver[2], Xingjie Lu[3], Bernard Pak[3], Xiaogu Zheng[1]

[1]College of Global Change and Earth System Science, Beijing Normal University, Beijing, China

[2]School of Earth Sciences, University of Melbourne, Melbourne, Australia

[3]CSIRO Ocean and Atmosphere, Aspendale, Victoria 3195, Australia

Correspondence to: Y. P. Wang, CSIRO Ocean and Atmosphere, Aspendale, Vic 3195, Australia, (Yingping.Wang@csiro.au)

## Abstract

Changes in atmospheric $CO_2$ levels, surface temperature or precipitation have been identified to have significantly contributed to the estimated increase in the terrestrial carbon-uptake rate over the last few decades, however those analyses did not consider the interactions. Using the Australian community land surface model (CABLE), we performed factorial experiments to quantify the importance of external drivers (climate drivers and atmospheric $CO_2$) and their interactions on annual terrestrial carbon uptake ($F_L$), excluding land-use change and fires, from 1959 to 2013. Our model simulations show a trend of 0.025 ±0.015 Pg C $yr^{-2}$ (or ~1.5% $yr^{-1}$) in global $F_L$ for 1959-2013, which is largely attributed to the positive influences of the increased atmospheric $CO_2$ (0.050± 0.001 Pg C $yr^{-2}$) and negative influences of changes in climate (-0.026 ± 0.014 Pg C $yr^{-2}$). Globally contribution of the nonlinear effects of dominant drivers to the simulated trend in $F_L$ is small (<10%), but can be significant regionally (>35%), particularly in the boreal forests and semi-arid regions. The interactions between temperature and $CO_2$ or temperature and precipitation can dominate the simulated trend in parts of Europe, south-eastern North America, southern China and some semi-arid regions. This modelling result suggests that the effects of nonlinear interactions of drivers on the trend of land carbon uptake should be considered in future studies.




## 1. Introduction

Recent studies have shown that the increase in atmospheric $CO_2$ concentration accounts for about 60% of the estimated global land carbon uptake [e.g. *Schimel et al.*, 2015; *Friend et al.*, 2014; *Ciais et al.*, 2013]. While increasing atmospheric $CO_2$ in the past had significant impacts on the mean global land carbon uptake, inter-annual variation in surface air temperature and precipitation were found to be the dominant drivers of inter-annual variability in global land uptake [*Poulter et al.*, 2014; *Ahlström et al.*, 2015]. Using modelling results, *Ahlström et al.* [2015] provide further evidence that semi-arid ecosystems dominated both the trend and inter-annual variability of the global terrestrial carbon sink over the past three decades, because of their strong sensitivities in photosynthetic carbon uptake to

precipitation and temperature. *Nemani et al.* (2003) found that net primary production of the global land biosphere for the period 1982-1999 increased at a rate of 6.17% per year, with highest rates in the water- and radiation-limited regions at high latitudes and tropics of the Northern Hemisphere. *Shaw et al.* [2002] show that increased $CO_2$ suppressed the effects of increased temperature, precipitation on annual net primary production (NPP) in Californian grassland. That result indicated that the combined effects of external drivers (climate drivers and atmospheric $CO_2$) differ greatly from linear combinations of individual responses to the drivers. Manipulative experiments analysis [*Wu et al.*, 2011] showed that warming and increased precipitation can stimulate plant growth and ecosystem carbon uptake whereas decreased precipitation has the opposite effects. A corollary of these findings is that multiple climate drivers jointly affect carbon-cycle processes in terrestrial ecosystems, and it is reasonable to expect that their nonlinear interactions may be important. Studies have shown that photosynthetic carbon production and ecosystem respiration vary with atmospheric $CO_2$, air temperature and precipitation nonlinearly [e.g. *Schimel et al.*, 2001; *Norby et al.*, 2004; *Arnone et al*., 2008; *Luo et al.*, 2008; *Phillips et al.*, 2009; *Leuzinger et al.*, 2011; *Wang et al.*, 2013], and that air temperature, precipitation and other climate variables often co-vary [*Jones and Humle*, 1996].

Previous studies examining the contribution of different forcings on regional or global land carbon uptake have only analysed the individual effects of those forcings. (see *Nemani et al.*, 2003; *Piao et al.*, 2013; *Poulter et al.*, 2014; *Ahlström et al.*, 2015]. For instance, *Piao et al.* [2013] applied multiple linear regression methods using temperature, precipitation and $CO_2$ concentration as independent variables to model the response of gross primary productivity (GPP) and net biome production (NBP) from process-based terrestrial ecosystem models and observations, and did not explicitly estimate the interactions among external drivers. Furthermore the first-order effects on the annual carbon uptake of some variables, such as increased $CO_2$ and temperature or precipitation can be opposite. The net effect on net land carbon uptake may therefore strongly depend on the interactions between such drivers.

In this study, we used a process-based global land surface model to quantify contributions of the changes in eight external drivers (seven key climate driving variables and increased $CO_2$ concentration) and their interactions to the simulated trend in annual terrestrial carbon uptake for the period 1959-2013. We performed a number of numerical simulations using the Australian community land surface model (CABLE) with CRUNCEP v5 forcing data. Firstly, we assessed the capability of CABLE in simulating change in land carbon uptake, ignoring effects from land use change and fires, over the historical period (1959-2010) by comparing with the estimates from the Global Carbon Project (GCP) [*Le Quéré et al.*, 2014] and TRENDY models (a comprehensive inter-comparison of process-based terrestrial ecosystem models) [*Piao et al.*, 2013; *Sitch et al.*, 2015]. Secondly, we designed a group of CABLE simulations to attribute the individual and pairwise contributions of individual

climate variables and $CO_2$ concentration to the trend in simulated terrestrial carbon uptake from 1959 to 2013. Finally, we discuss how trend analysis without considering the nonlinear effects may incorrectly attribute the simulated trend of regional carbon uptake.

# 2. Methods

### 2.1 CABLE v2 model and forcing datasets

The Australian Community Atmosphere Biosphere Land Exchange (CABLE) model version 2 is a global land-surface model for terrestrial biophysical and biogeochemical processes [*Wang et al.*, 2010, 2011; *Kowalczyk*, 2006]. The model consists of 5 sub-models: radiation, canopy micrometeorology, surface flux, soil and snow, and biogeochemical cycles. CABLE has been benchmarked against other terrestrial ecosystem models using observations from eddy flux measurements [*Best et al.*, 2015]; manipulated field experiments [*De Kauwe et al.*, 2014], regional to global observations [*Piao et al.*, 2015] using offline simulations. These studies have shown that CABLE generally performs well compared to other process-based land surface models.

CABLE is forced by seven meteorological forcing variables (temperature, precipitation, downward short-wave radiation, downward long-wave radiation, specific humidity, pressure, wind speed – these are later abbreviated as *T*, *R*, *S*, *L*, *Q*, *P* and *W*, respectively) and surface $CO_2$ concentration (abbreviated as *C*). CRUNCEP version 5 [*New et al.*, 2002; *New and Jones*, 1999, 2000] meteorological 6-hourly forcing dataset was used in this study. CRUNCEP is a combination of (i) the CRU TS.3.22 0.5° × 0.5° monthly climatology covering the period 1901–2013 [*Mitchell and Jones*, 2005], and (ii) the 6-hourly NCEP reanalysis 2.5° × 2.5° climatology covering the period 1948 to 2013 [*Kalnay et al.*, 1996]. CRUNCEP dataset was interpolated to hourly time series so that can be used as input to CABLE. The annual mean of global surface $CO_2$ concentration during 1901-2013 was used, which was reconstructed from the combination of ice core records in the Antarctic and atmospheric observations since the late 1950s [*Keeling and Whorf*, 2005].

All simulations in this study were performed with carbon, nitrogen and phosphorous cycles to account for possible limitations of nitrogen and phosphorous on land carbon uptake [*Wang et al.*, 2009; *Zhang et al.*, 2011; *Goll et al.*, 2012] and the canopy leaf area index (LAI) was dynamically predicted. The importance of including both nitrogen and phosphorous limitation for accurately representing biogeochemical cycles in CABLE has been discussed before [See *Zhang et al.*, 2013, 2014; *Wang et*

*al.*, 2015]. Land-use change and disturbances, such as fires, are not included. The vegetation cover of 1990 was used for all simulations. To obtain the initial sizes of all carbon, nitrogen and phosphorous pools, we used the semi-analytical solution (SAS) method to accelerate the spin-up of CABLE to steady state of coupled carbon-nitrogen-phosphorus processes [*Xia et al.*, 2012] forced by CRUNCEP data from 1901 to 1910 and an atmospheric $CO_2$ concentration of 296.64 ppm (i.e. 1901 level).

**2.2 Experimental design**

To isolate the influences of individual drivers (physical climate variables and surface $CO_2$ concentration) on the annual land-carbon uptake (i.e. net ecosystem productivity, or NEP), we performed a number of simulations from 1901 to 2013. Firstly, we calculated the climatology of each climate variable as follows: (1) by averaging all hourly data for the variable at the same hour of the same day-of-year from CRUNCEP climate forcing over 1901-2013; (2) applying the averaged data of that variable as a new forcing variable for each year over 1901-2013 repeatedly. This time series of the climatology has no inter-annual variation and no trend, but maintains the mean diurnal and seasonal variations of the original time series, and is used as the climatology of that climate variable. This is done for each of seven climate variables. For atmospheric $CO_2$, we used either a constant atmospheric $CO_2$ fixed at 296.64 ppm (1901 level) or historical $CO_2$ concentration as used in the CMIP5 (Coupled Model Inter-comparison Project Phase 5) simulations [*Taylor et al.*, 2012].

We assume that the contribution of a driving variable to NEP may consist of its direct effect (first order effect) and interactions (second order effect or higher) with each of other seven driving variables. The effects of driving variables $X$=($C$, $T$, $R$, $S$, $L$, $Q$, $P$, $W$) on the trend of NEP, $f(X)$ can be written in the following form:

$$f(X) = f_0 + \sum_{i=1}^{n} f_i(x_i) + \sum_{1 \le i < j}^{n} f_{i,j}(x_i, x_j) + \varepsilon \qquad (1)$$

where $n$=8, and $f_i(x_i)$ is the first-order effect of $x_i$ (climate variables and $CO_2$) on $f(X)$, and $f_{i,j}(x_i, x_j)$ is a second-order effect resulting from the interaction of $x_i$ and $x_j$ on $f(X)$, and $\varepsilon$ is the residual error term that includes higher order effects. Usually higher-order effects (>2) are weak and then can be neglected [*Ziehn and Tomlin*, 2009]. The overall trend appears as $f(X)$, while $f_0$ is the baseline trend such that each driver is set to its climatology (n.b. it can be seen that $f_0 = 0$ after the model spin-up). This approach is based upon the same decomposition of the response function as used in variance-based sensitivity analysis [e.g. *Saltelli et al.*, 2008, section 4.3].

Using the initial carbon pool sizes obtained from the model spin-up, we performed the following simulations: (i) normal run (historical simulation), forced by the original CRUNCEP climate and historical $CO_2$; (ii) climate only, forced by the original CRUNCEP climate and fixed $CO_2$ at 1901 level; (iii) $CO_2$ only simulation, forced by the climatologies of all climate variables and historical $CO_2$; (iv) seven individual climate variable simulations for estimating each first-order effect forced by the original values for one climate variable while using the climatologies for other six climate variables and the fixed $CO_2$; (v) 21 simulations to quantify interactions between two variables, forced by the two original (non-detrended) climate variables and using climatologies for the other five climate variables and fixed $CO_2$; (vi) seven $CO_2$ × climate variable simulations. This is the same as (iv) but with historical $CO_2$. In total we conducted 38 CABLE simulations from 1901 to 2013 (see Table 1). We note that simulation groups (iii) to (vi) represent the set of all one- and two- factor interactions. To estimate the contribution of variability in temperature, for example, to the trend in the state variable NEP of CABLE, we can calculate the first-order temperature effect as $f_2(T)$ ($NEP^{T\_FO\_fix\_CO2}$ in simulation set iv) and the interaction effects between temperature and the other driving variables such as $f_{1,2}(T,C)$, $f_{2,3}(T,R)$, $f_{2,4}(T,Q)$ etc., following Eq. 1. The effect on NEP from the interaction such as between *T* and *R* $f_{2,3}(T,R)$ was defined as the difference in NEP from the interaction simulation between *T* and *R* ($NEP^{T\_R\_SO\_fix\_CO2}$ in simulation set v) and the first-order simulation of *T* and of *R*: $f_{2,3}(T,R) = NEP^{T\_R\_SO\_fix\_CO2} - NEP^{T\_FO\_fix\_CO2} - NEP^{R\_FO\_fix\_CO2}$.

Finally, we can calculate each variable's first order effect and their second order effects. The total effect is the sum of all first order effects and second order effects (Eq. 1).

## 3. Results

We consider the study period 1959-2013, so as to compare our model results with data from the Global Carbon Project (GCP), which covers the same period. We also compare our results with the TRENDY ensemble data, which spans 1959-2010. The estimates of GCP are the residual land sinks of fossil fuel and land-use and fires net emissions, the growth rate in atmospheric $CO_2$ concentration and the oceanic $CO_2$ sink, based on mass-balance [*Le Quéré et al.*, 2013]. The TRENDY dataset in this study is made up of an ensemble of seven process-based terrestrial ecosystem model simulations (TRENDY experiment S2 without land-use change and fires including CLM4C, CLM4CN, LPJwsl, LPJ-GUESS, OCN, SDGVM, TRIFFID here)[*Piao et al.*, 2013]. Our modeling study only focused on the natural response of the terrestrial ecosystem and did not account for land-use change and fires which are largely explained by historical human activities. The contribution of fires and land-use change to the

trend has been estimated by the GCP at -0.008 ±0.001 Pg C $yr^{-2}$ for the period of 1959-2013 [*Le Quéré et al.*, 2014], which is small relative to the trend in NEP (see below). Here the comparison with the residual land-sink from the GCP and results from TRENDY is mainly as an informative benchmark. We firstly compared the estimated trend in annual NEP (land carbon uptake) by CABLE (the normal run) with that of the GCP and the TRENDY model ensemble, and then analyze the linear and nonlinear effects of changes in atmospheric $CO_2$ and climate variables on the simulated trend by CABLE.

Figure 1 shows that global annual land carbon uptake ($F_L$) simulated by CABLE with varying $CO_2$ and climate is consistent with the estimates of the GCP from 1959 to 2013 ($R^2$=0.65) and the TRENDY ensemble mean ($R^2$=0.87). The modeled $F_L$ from CABLE has a mean sink of 2.079 Pg C $yr^{-1}$, with a trend of 0.028 ± 0.017 Pg C $yr^{-2}$ for 1959-2010, as compared to the estimated mean sink of 2.026 Pg C $yr^{-1}$ and trend of 0.020 ± 0.009 Pg C $yr^{-2}$ from GCP, and a mean of $F_L$ of 1.684 Pg C $yr^{-1}$ and trend of 0.035 ± 0.007 Pg C $yr^{-2}$ from the ensemble TRENDY model simulations over the same period.

Comparing the differences in the simulated trends by CABLE with fixed $CO_2$ or fixed climate, we found that increased $CO_2$ contributed to a positive trend in $F_L$ of 0.050± 0.001 Pg C $yr^{-2}$ but very little to the inter-annual variation in $F_L$ (std.dev. = 0.48 Pg C $yr^{-1}$), while the climate variations dominated the inter-annual variability in $F_L$ and led to a significant negative trend in $F_L$ of -0.026 ± 0.014 Pg C $yr^{-2}$.

Using the full set of simulations we were able to attribute the influence of climate change and atmospheric $CO_2$ increase in the simulated trend in $F_L$. At a global scale, the estimated trend in $F_L$ by CABLE is about 0.025 ±0.015 Pg C $yr^{-2}$, which is largely due to the positive influencess of the increased atmospheric $CO_2$ from 316 to 395 ppm for the period 1959-2013 as well as greater precipitation and specific humidity, and the negative influences of increasing surface temperature and longwave radiation over this period (Figure 2a). Globally, the impacts of $CO_2$ and climate variables on the simulated trend in $F_L$ are dominated by their linear effect (93%), and the nonlinear effects are relatively small (7%).

The same analysis can be performed both regionally and for areal classifications, such as land cover. Among the different plant functional types (PFTs), evergreen broad-leaf forests (EBF) are the largest contributor (about 0.015 Pg C $yr^{-2}$) to the overall trend in $F_L$ simulated by CABLE over 1959-2013 (Figure 2b). Contributions from evergreen needle-leaf forests (ENF), deciduous broad-leaf forests (DBF), $C_4$ grassland and crop are small (about 0.0025 Pg C $yr^{-2}$ respectively), and the deciduous needle-leaf forests (DNF), shrub, $C_3$ grassland and tundra land do not show any significant trends in $F_L$. Across all PFTs, the increased $CO_2$ is the largest positive contributor, and temperature has the largest

negative impact. The overall trend for each PFT is a relatively small value, which is the sum of both positive and negative linear effects and interaction terms. The interactions can be positive or negative for different PFTs, and were found to be larger than the overall simulated trend in $F_L$ for ENF, DNF, Shrub, $C_3$, $C_4$ and Crop and thus can determine the sign of the overall value of trend in $F_L$ in such cases.

While the overall trend at global or PFT-scale is always positive, the trend is much more variable regionally. Figure 3a shows that for the normal run (varying climate and $CO_2$) over 1959-2013, several regions have large positive trends in $F_L$ of more than 1.00 g C $m^{-2}$ $yr^{-2}$. These include the non-central areas of Amazonian forests, and eastern Indonesian forest, where it is likely caused by fertilization of the increased $CO_2$ concentration, which contributes more than 35% of the overall contribution and is larger than influences of other variables (see Figure 3b). The areas with a significant negative trend of less than 1.00 g C $m^{-2}$ $yr^{-2}$ are distributed through southeastern North America and Eastern Europe, where surface air temperature is the largest negative contributor with more than 35% of the total contribution. In addition, most of the semi-arid regions are mainly affected by changes in precipitation, which account for between 15%-35% of the overall trend in these regions (Figure 3b).

At regional scales, interactions such as between $CO_2$ and temperature, $CO_2$ and precipitation, or temperature and precipitation can have significant effects on the simulated trend in $F_L$ by CABLE (Figure 3c and 3d). Figure 3c shows the ratio of the combined interaction terms to the total trend in $F_L$ of the normal run (Figure 3a). Figure 3d shows the ratio of the dominant interactions to the total trend in $F_L$ of the normal run. The dominant interactions can contribute >35% of total interactions effects regionally. The other interactions such as between wind speed (or pressure) and other variables can be ignored (<5% of total interactions), but interactions between temperature and shortwave radiation (or longwave radiation, humidity etc.) can also averagely contribute about -35%~35% of total interactions effects at regional scales. As the trend in $F_L$ of the normal run (Figure 3a) in regions can be negative or positive, so the fractions or ratios due to interactions can also be negative or positive. For example, in some regions such as Eastern Europe, south-eastern North America and southern China, fractions of interactions effect are less than -100% (Figure 3c), while the trends in $F_L$ of the normal run are negative (Figure 3a). It means that in these regions, interactions among driving variables made a large positive contribution to the overall trend in $F_L$. In these regions (Figure 3d), the dominant interactions between $CO_2$ and temperature or between temperature and precipitation have positive effects. In semi-arid regions, the strong interaction between temperature and precipitation can be either positive such as southern Africa or negative such as eastern Australia, and this interactive effect on the simulated trend in $F_L$ can also be larger than the trend in $F_L$ from the normal run (Figure 3d). However, interactive

effects are not significant in tropical rainforests. In other words the trend in $F_L$ for tropical rainforests is mostly dominated by the linear effect of the individual external drivers.

## 4. Discussion

The most important result of our factorial experiments is that interactions or synergies among driving variables are significant drivers of regional trends in carbon uptake. The study must be regarded as exploratory since it is carried out with a model and inherits the associated weaknesses. This could be partially addressed with an extension of previous intercomparison studies to include a subset of the interactions considered here. The result does raise a number of further questions which take us beyond our scope in this paper.

Firstly, the response to a forcing is composed of the size of the forcing and the sensitivity of the system to it. This holds as much for combined as single forcings. Are the regional differences we see in responses a product of differences in forcing or sensitivity? Secondly the net uptake we have studied is the difference between ecosystem respiration and assimilation. Can we attribute the regional responses to either of these gross fluxes in particular? Such a study would need to consider carefully the coupling between respiration and assimilation via the carbon pools.

Finally and most importantly we should test the conclusion with observations. Here we can make some headway using previous studies. *Field et al.* [1995] found that increased $CO_2$ causes most plants to save water by reducing stomatal conductance. Thus increased $CO_2$ can mitigate negative effects of drought, and stimulate plant growth in water-limited conditions, leading to the positive interaction between temperature and increased $CO_2$ [*Holtum and Winter*, 2010; *Morgan et al.*, 2006; *Nemani et al.*, 2003]. The Arizona free-air $CO_2$ enrichment (FACE) experiment has shown that biomass growth and many plant physiological processes were interactively affected by the combination of increased $CO_2$ and altered water availability [*Kimball et al.*, 2001; *Wall et al.*, 2006]. *Luo et al.* [2008] showed that the positive (or negative) interaction between increased temperature and altered precipitation were due to the enhanced (or reduced) soil water availability that is linked to the response of water-limited ecosystem to warming [*Gerten et al.*, 2008]. As is shown in our findings, interactions in tropical forests were not significant, partly because the tropical forests are not water-limited systems. In the future, more studies of experimental evidence and mechanisms for the interactive effects on such as primary productivity and ecosystem respiration are needed to in-depth explain non-linear interactive effects on trend in net land carbon uptake.

Among the previous studies of historical trends in global land carbon uptake, few modelling studies have attributed causes of these changes to individual climate drivers (*Nemai et al.*, 2003; *Poulter et al.*, 2014; *Ahlström et al.*, 2015), and to our knowledge none have quantified the contribution from non-linear interactions among climate drivers. Further measurement field experimental studies for ecosystem response of typical plant classifications to multiple climate factors (not only single-factor experiments) are also needed, though such long-term experiments are relatively expensive and hence uncommon. In addition, land use changes due to deforestation, afforestation and forest regrowth should also be taken into account when verifying these findings with observations from surface sites or satellites, as land use changes has become a significant contributor especially in boreal regions such as Europe [*FAO*, 2010; *Le Quéré et al.*, 2014]. Overall, this study on attribution of trend in terrestrial carbon uptake has quantified the relative importance of the main drivers and their interactions, and thereby adds to our understanding of interactive effects in the global carbon cycle and climate change.

## Acknowledgements

We thank the China Scholarship Council for the financial support to Xuanze Zhang. P. Rayner was partly supported by an Australian Professorial Fellowship (DP1096309). J. Silver was supported by a McKenzie Postdoctoral Fellowship from the University of Melbourne. This research was undertaken with the assistance of resources from the National Computational Infrastructure (NCI), which is supported by the Australian Government. The GCP and TRENDY data used here are downloaded at http://www.globalcarbonproject.org/reccap/products.htm.

## References

Ahlström, A., et al. (2015), Carbon cycle. The dominant role of semi-arid ecosystems in the trend and variability of the land CO(2) sink, *Science*, 348(6237), 895-899.

Arnone, J. A., et al. (2008), Prolonged suppression of ecosystem carbon dioxide uptake after an anomalously warm year, *Nature*, 455(7211), 383-386.

Ciais, P., et al. (2013), Carbon and other biogeochemical cycles. Climate Change 2013. The Physical Science Basis. Contribution of Working Group I to the Fifth Assessment Report of the Intergovernmental Panel on Climate Change, eds Stocker TF, et al. (Cambridge Univ Press, New York), pp 465–570.

FAO (2010), Global Forest Resource Assessment 2010, 378 pp.

Field, C. B., R. B. Jackson, and H. A. Mooney (1995), Stomatal responses to increased $CO_2$ – implications from the plant to the global scale, *Plant Cell Environ.*, 18, 1214–1225.

Friend, A. D, et al. (2014), Carbon residence time dominates uncertainty in terrestrial vegetation responses to future climate and atmospheric $CO_2$, *Proc. Natl. Acad. Sci. U.S.A.*, 111(9), 3280–3285, doi:10.1073/pnas.122247711.

Goll, D. S., et al. (2012), Nutrient limitation reduces land carbon uptake in simulations with a model of combined carbon, nitrogen and phosphorus cycling, *Biogeosciences*, 9, 3547-3569, doi:10.5194/bg-9-3547-2012.

Gerten, D., et al. (2008), Modelled effects of precipitation on ecosystem carbon and water dynamics in different climatic zones, *Global Change Biol.*, 14(10), 2365-2379.

Holtum, J.A.M. and Winter, K. (2010), Elevated [CO2] and forest vegetation: more a water issue than a carbon issue? *Funct. Plant Biol.*, 37, 694–702.

Jones, P. D., and M. Hulme. (1996), Calculating regional climatic time series for temperature and precipitation: methods and illustrations, *Int. J. Climatol.*, 16(4), 361-377.

Kalnay, E., et al. (1996), The NCEP/NCAR 40-Year Reanalysis Project, *Bull. Amer. Meteor. Soc.*, 77, 437–471.

Keeling, Charles D., and Timothy P. Whorf. (2005), Atmospheric CO2 records from sites in the SIO air sampling network, *Trends: a compendium of data on global change*, 16-26.

Kimball, B. A., et al. (2001), Elevated CO2, drought and soil nitrogen effects on wheat grain quality, *New Phytologist*, 150, 295–303.

Kowalczyk, E. A. (2006), The CSIRO Atmosphere Biosphere Land Exchange (CABLE) model for use in climate models and as an offline model, *CSIRO Marine and Atmospheric Research* 013.

Le Quéré, C., et al. (2013), The global carbon budget 1959–2011, *Earth System Science Data*, 5, 165-185.

Le Quéré, C., et al. (2014), Global carbon budget 2013, Earth System Science Data, 6, 235-263.

Leuzinger, Sebastian, Yiqi Luo, Claus Beier, Wouter Dieleman, Sara Vicca, and Christian Körner. (2011), Do global change experiments overestimate impacts on terrestrial ecosystems? *Trends Ecol. Evol.*, 26(5), 236-241.

Luo, Y., et al. (2008), Modeled interactive effects of precipitation, temperature, and [$CO_2$] on ecosystem carbon and water dynamics in different climatic zones, *Global Change Biol.*, 14, 1986–1999.

Mitchell, T. D., and P. D. Jones (2005), An improved method of constructing a database of monthly climate observations and associated high-resolution grids, *Int. J. Climatol.*, 25(6), 693-712.

Morgan, J. A., et al. (2006), Water relations in grassland and desert ecosystems exposed to elevated atmospheric CO2, *Oecologia*, 140, 11–25.

Nemani, R. R., et al. (2003), Climate-Driven Increases in Global Terrestrial Net Primary Production from 1982 to 1999, *Science*, 300(5625), 1560-1563, doi:10.1126/science.1082750.

New, M., M. Hulme and P. Jones (1999), Representing twentieth-century space-time climate variability. Part I: Development of a 1961−90 mean monthly terrestrial climatology, *J. Clim.*, 12, 829–856.

New, M., M. Hulme, and P. Jones (2000), Representing twentieth-century space-time climate variability. Part II: Development of 1901−1996 monthly grids of terrestrial surface climate, *J. Clim.*, 13, 2217–2238.

New, M., D. Lister, M. Hulme, and I. Makin (2002), A high-resolution data set of surface climate over global land areas, *Clim. Res.*, 21, 1–25.

Phillips, O. L., et al. (2009), Drought sensitivity of the Amazon rainforest, *Science*, 323(5919), 1344-1347.

Piao, S. L., et al. (2015), Detection and attribution of vegetation greening trend in China over the last 30 years, *Global Change Biol.*, 21, 1601–1609, doi:10.1111/gcb.12795.

Piao, S. L., et al. (2013), Evaluation of terrestrial carbon cycle models for their response to climate variability and to CO2 trends, *Global Change Biol.*, 19(7), 2117-2132, doi:10.1111/gcb.12187.

Poulter,B., et al. (2014), Contribution of semi-arid ecosystems to interannual variability of the global carbon cycle, *Nature*, 509, 600-603.

Saltelli, A., M. Ratto, T. Andres, F. Campolongo, J. Cariboni, D. Gatelli, M. Saisana, and S. Tarantola (2008), Global sensitivity analysis: the primer, John Wiley & Sons.

Schimel, D., B. B. Stephens, and J.B. Fisher (2015), Effect of increasing CO2 on the terrestrial carbon cycle, *Proc. Natl. Acad. Sci. U.S.A.*, 112(2), 436-441.

Schimel, D. S., et al. (2001), Recent patterns and mechanisms of carbon exchange by terrestrial ecosystems, *Nature*, 414(6860), 169-172.

Sitch, S., et al. (2015), Recent trends and drivers of regional sources and sinks of carbon dioxide, *Biogeosciences*, 12, 653-679, doi:10.5194/bg-12-653-2015.

Taylor, K. E., R. J. Stouffer, and G. A. Meehl (2012), An Overview of CMIP5 and the Experiment Design, *Bull. Amer. Meteor. Soc.*, 93, 485–498, doi:10.1175/BAMS-D-11-00094.1.

Wall, G.W., et al. (2006), Interactive effects of elevated carbon dioxide and drought on wheat, *Agron. J.*, 98, 354–381.

Wang, W., et al. (2013), Variations in atmospheric CO2 growth rates coupled with tropical temperature, *Proc. Natl. Acad. Sci. U.S.A*, 110 (32), 13061-13066, doi:10.1073/pnas.1219683110.

Wang, Y. P. and B. Houlton (2009), Nitrogen constraints on terrestrial carbon uptake: Implications for the global carbon-climate feedback, *Geophys. Res. Lett.*, 36, L24403, doi:10.1029/2009GL041009.

Wang, Y. P., R. M. Law and B. Pak (2010), A global model of carbon, nitrogen and phosphorus cycles for the terrestrial biosphere, *Biogeosciences*, 7, 2261–2282, doi:10.5194/bg-7-2261-2010.

Wang, Y. P., E. Kowalczyk, R. Leuning, G. Abramowitz, M. R. Raupach, B. Pak, E. van Gorsel, and A. Luhar (2011), Diagnosing errors in a land surface model (CABLE) in the time and frequency domains, *J. Geophys. Res.*, 116, G01034, doi:10.1029/2010JG001385.

Wang, Y.P., Q., Zhang, A. Pitman, and Y. Dai (2015), Nitrogen and phosphorous limitation reduces the effects of land use change on land carbon uptake or emission, *Environ. Res. Lett.*, 10(1), 014001.

Xia, J., Y. Luo, Y. P. Wang, E. Weng and O. Hararuk (2012), A semi-analytical solution to accelerate spin-up of a coupled carbon and nitrogen land model to steady state, *Geosci. Model Dev. Discuss*., 5, 803-836.

Zhang, Q., Y.P., Wang, A. Pitman, and Y. Dai (2011), Limitations of nitrogen and phosphorous on the terrestrial carbon uptake in the 20th century, *Geophys. Res. Lett.*, 38, L22701.

Zhang, Q., A. J. Pitman, Y. P. Wang, Y. J. Dai, and P. J. Lawrence (2013), The impact of nitrogen and phosphorus limitation on the estimated terrestrial carbon balance and warming of land use change over the last 156 years, *Earth Syst. Dyn.*, 4, 333–345, doi:10.5194/esd-4-1-2013.

Zhang, Q., Y. P. Wang, R. J. Matear, A. J. Pitman, and Y. J. Dai (2014), Nitrogen and phosphorous limitations significantly reduce future allowable CO2 emissions, *Geophys. Res. Lett.*, 41, 632–637, doi:10.1002/2013GL058352.

Ziehn, T., and A.S. Tomlin (2009), GUI-HDMR – a software tool for global sensitivity analysis of complex models, *Environ. Model. Softw*., 24, 775–785, doi:10.1016/j.envsoft.2008.12.002.

**Table 1.** Experimental design of CABLE simulations

| Name | Abbrev | Climate | $CO_2$ | # Runs |
|---|---|---|---|---|
| **(i) Historical** | Hist **(normal run)** | Historical | Historical | 1 |
| **(ii) Climate only** | Clim_Only | Historical | Fixed | 1 |
| **(iii) $CO_2$ only** | $CO_2$_Only | Climatology | Historical | 1 |
| **(iv) X-first order** | X_FO_fix_$CO_2$ | Climatology for all but X | Fixed | 7 |
| **(v) X-Y second order** | X_Y_SO_fix_$CO_2$ | Climatology for all but X and Y | Fixed | 21 |
| **(vi) X-$CO_2$ second order** | X_$CO_2$_SO | Climatology for all but X | Historical | 7 |
| | | | Total = | 38 |

**Note that: X or Y (X≠Y) is one of the climate variables (*T, R, S, L, Q, P, W*).**

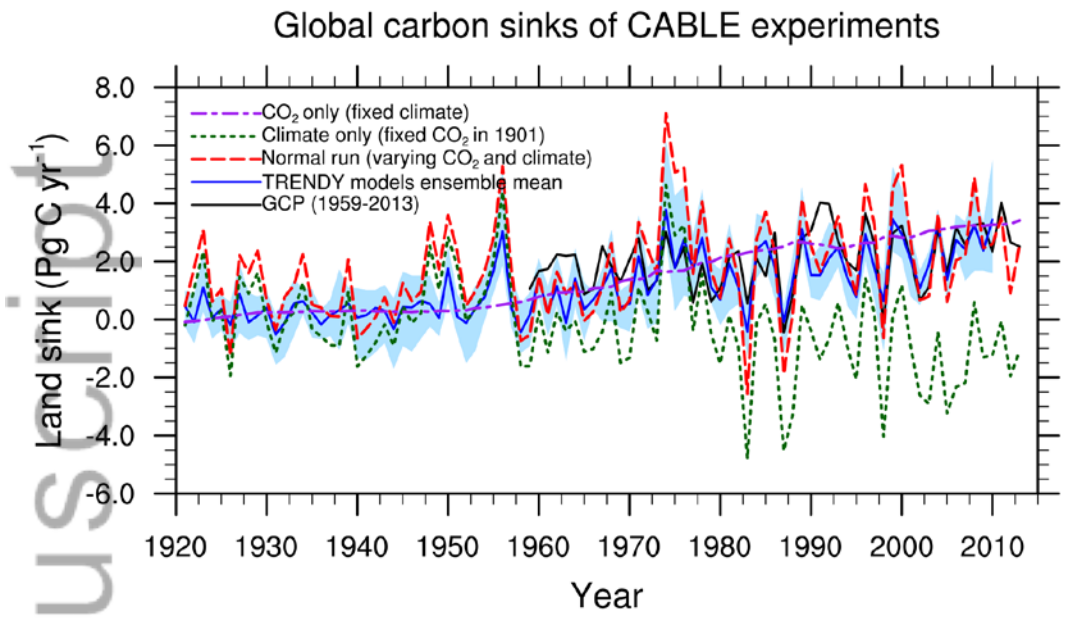


**Figure 1**. Timeseries of global annual land carbon uptakes (units: Pg C $yr^{-1}$) of sensitivity simulations by CABLE V2 from 1920 to 2013: normal run (varying $CO_2$ and varying climate), climate effect only (using fixed $CO_2$ at 1901 level), $CO_2$ effect only (using fixed climate averaged over 1901-2013), and land sink estimate of GCP from 1959 to 2013 (Le Quéré et al., 2013) and ensemble mean land sink from seven TRENDY models (CLM4C, CLM4CN, LPJwsl, LPJ-GUESS, OCN, SDGVM, TRIFFID) from 1920 to 2010 (Piao et al., 2013). The normal run was forced by a set of 6-hourly 0.5° × 0.5° CRUNCEP version 5 forcing data and historical atmospheric $CO_2$ concentration from 1901 to 2013. Note that these estimates did not consider land use change and fires effects.

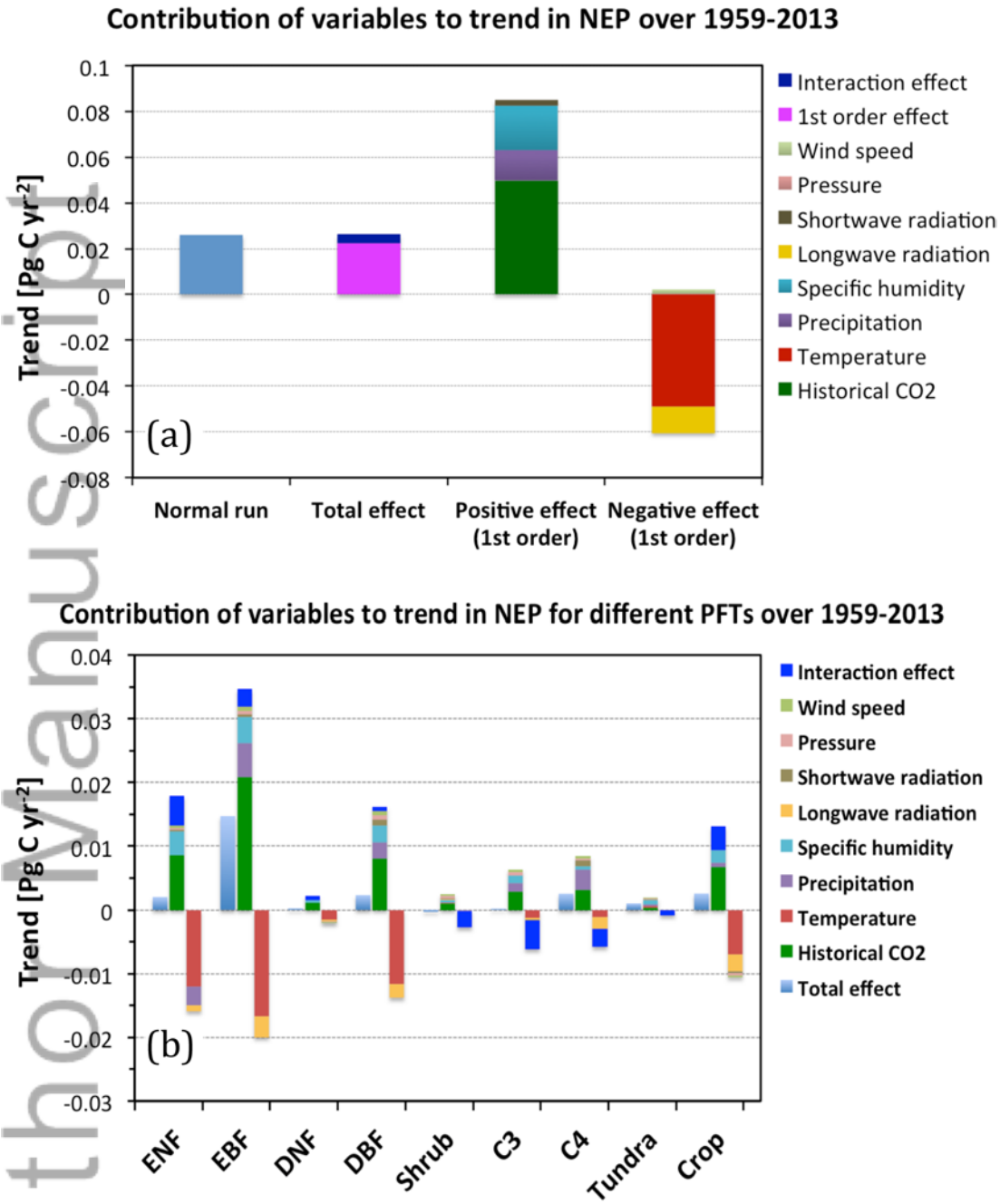


**Figure 2**. Contributions of external drivers (climate variables and surface $CO_2$) concentration to trends in annual land carbon uptake (or NEP) simulated by CABLE over 1959-2013: (a) for global land, and (b) for different plant functional types (PFTs) including evergreen needle-leaf forest (ENF), evergreen broad-leaf forest (NBF), deciduous needle-leaf forest (DNF), deciduous broad-leaf forest (DBF), shrub, C3 and C4 plant, crop and tundra.

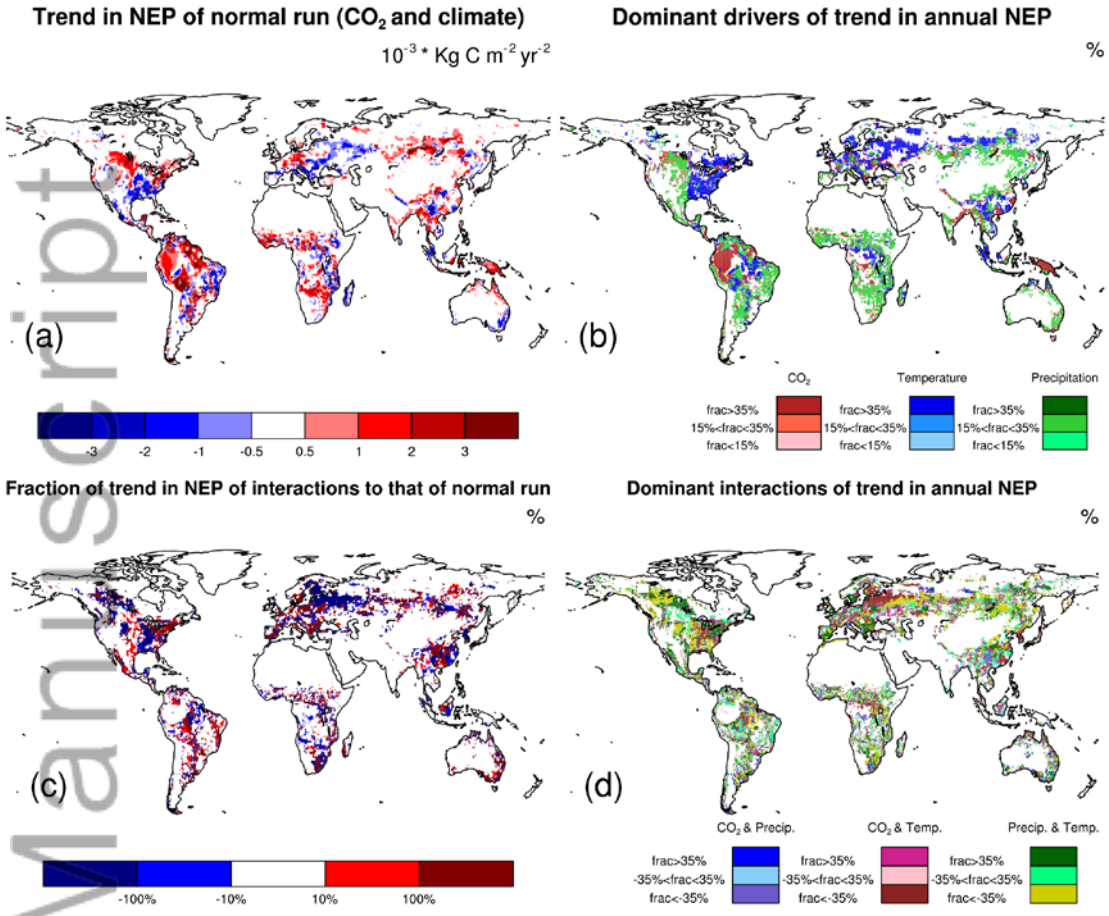


**Figure 3**. Spatial patterns of: (a) trend (Kg C $m^{-2}$ $yr^{-2}$) in annual land carbon uptake (NEP) from historical simulation (normal run) by CABLE v2 forced by climate and surface $CO_2$ concentration over 1959-2013; (b) contribution fraction (%) of trend in NEP due to dominant driving variables (temperature, precipitation, $CO_2$) to trend in annual NEP of normal run; (c) contribution fraction (%) of trend in annual NEP due to interactions among driving variables; (d) contribution fraction (%) of trend in annual NEP due to dominant interactions among driving variables (temperature, precipitation, $CO_2$). Note that the white areas in Fig. 3b (or Fig. 3d) correspond to white areas in Fig. 3a (Fig. 3c). Also, note that the contribution fraction is the ratio of trend in NEP due to interactions to trend in NEP of the normal run. Therefore, in Fig.3c and Fig.3d, in Eastern Europe and east-southern North American, for example, the significant negative values of fraction are due to the negative trend in NEP of normal run in the same areas (Fig. 3a).

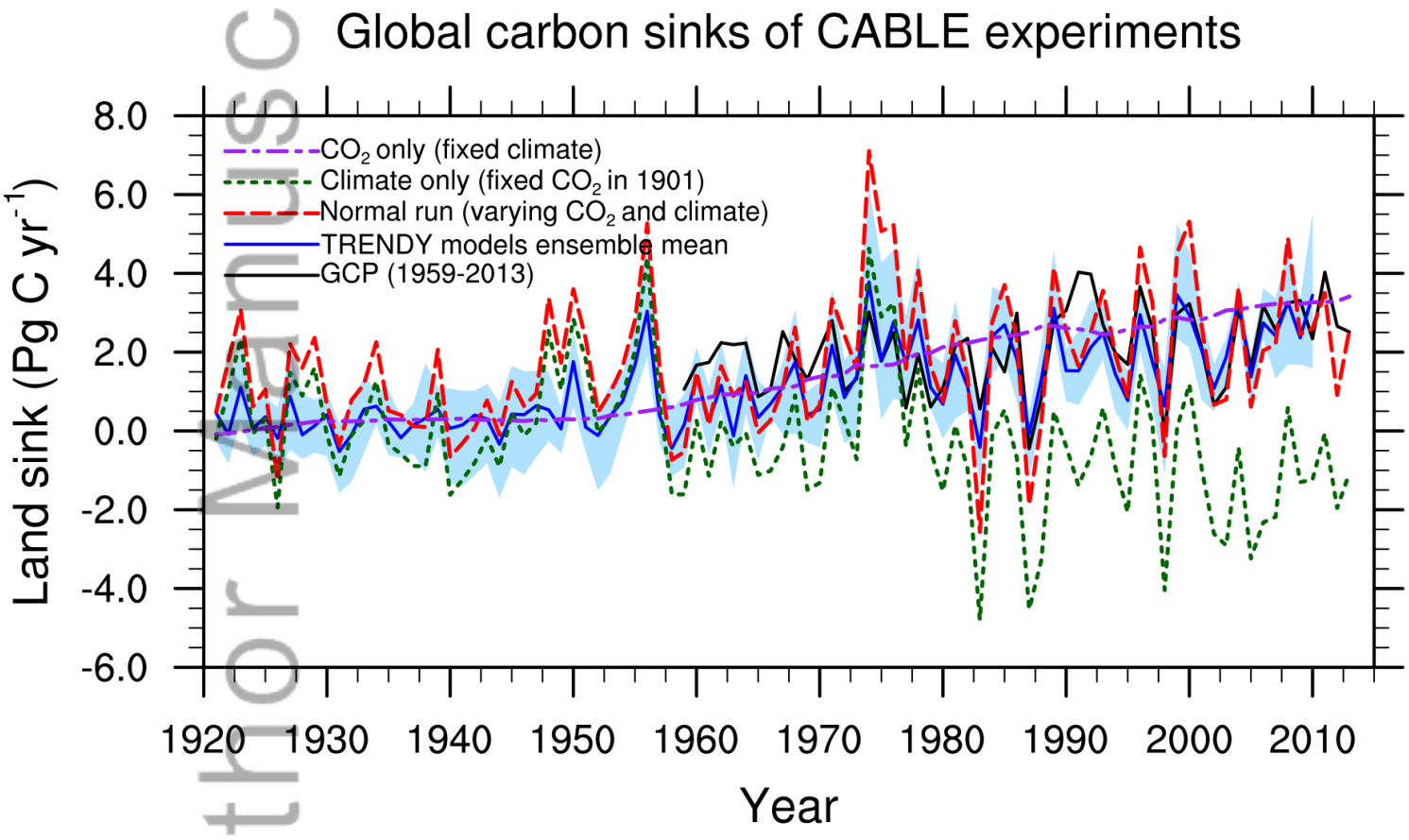


2015GL067162-f00-z-.png

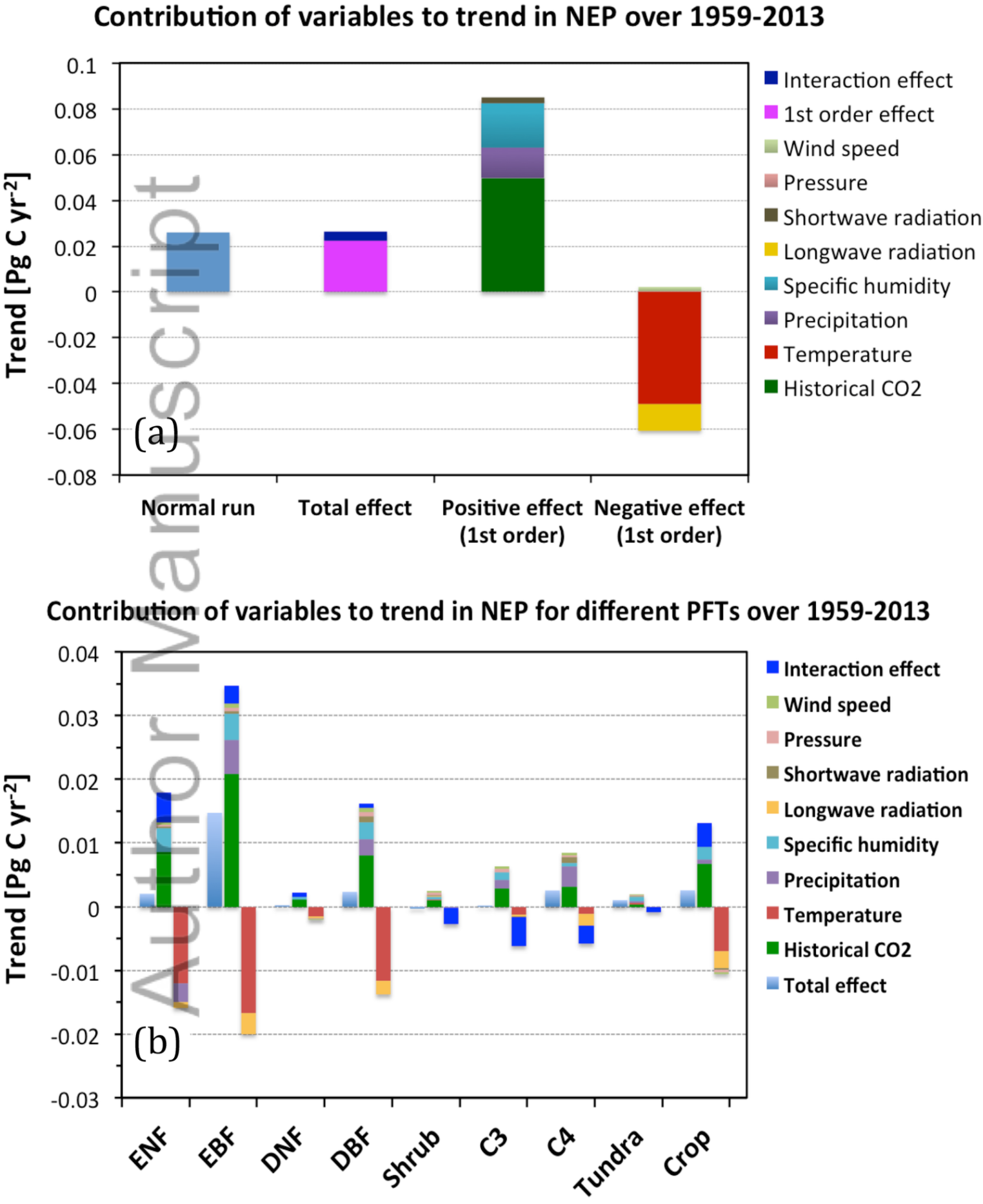




2015GL067162-f01-z-.png

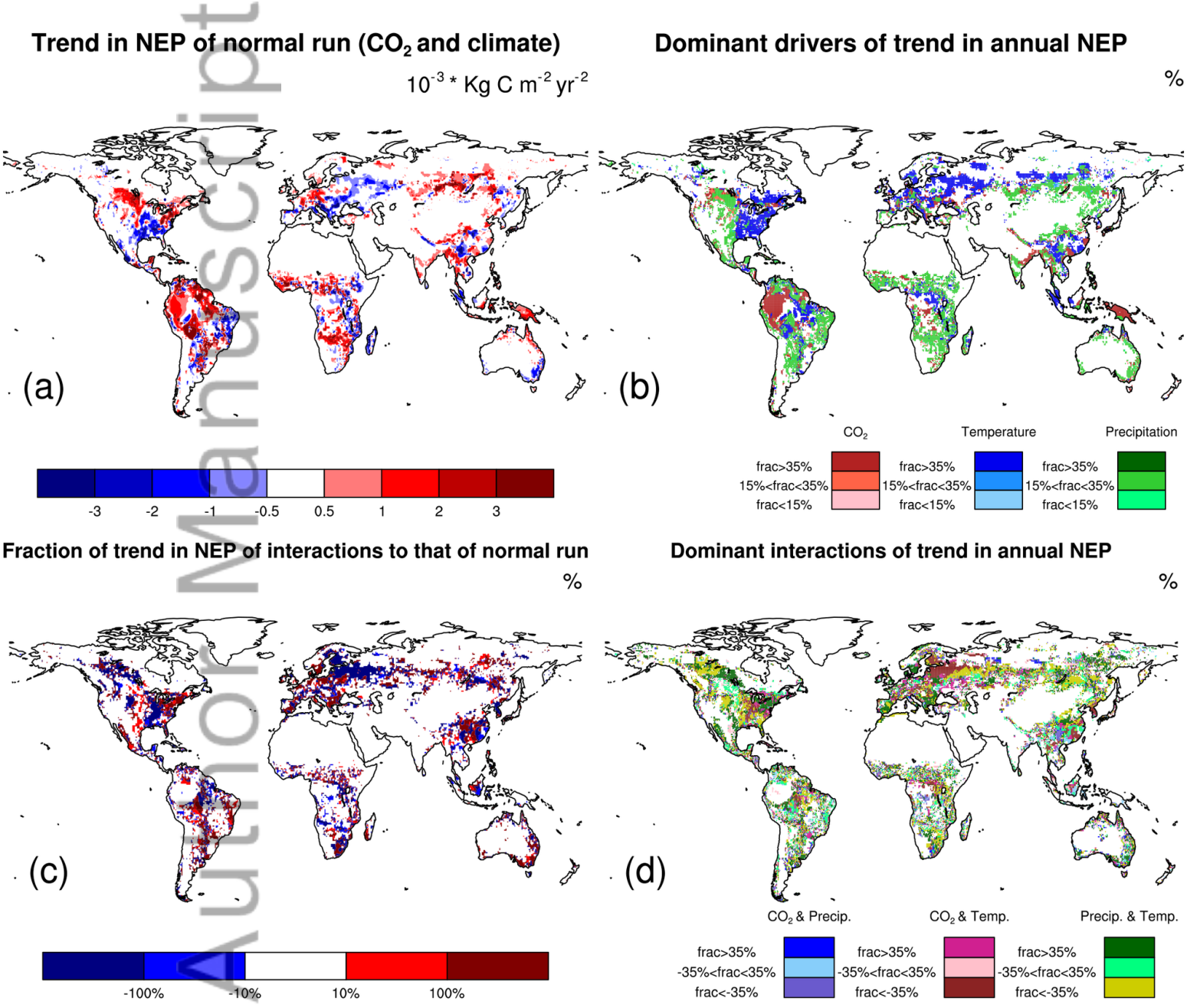


2015GL067162-f02-z-.png